IEEE Access
Multidisciplinary : Rapid Review : Open Access Journal

Received December 2, 2019, accepted January 2, 2020, date of publication January 10, 2020, date of current version January 24, 2020.

Digital Object Identifier 10.1109/ACCESS.2020.2965591

Generic System Frequency Response Model for Power Grids With Different Generations

H. HUANG[1], P. JU[2], (Senior Member, IEEE), Y. JIN[2], X. YUAN[1], (Senior Member, IEEE), C. QIN[2], (Member, IEEE), X. PAN[2], (Member, IEEE), AND X. ZANG[2]

[1]State Key Laboratory of Advanced Electromagnetic Engineering and Technology, School of Electrical and Electronic Engineering, Huazhong University of Science and Technology, Wuhan 430074, China
[2]College of Energy and Electrical Engineering, Hohai University, Nanjing 210098, China

Corresponding author: P. Ju (pju@hhu.edu.cn)

This work was supported in part by the National Natural Science Foundation of China under Grant 51837004, and in part by the 111 Project under Grant B14022.

ABSTRACT With the increasing integration of renewable generation, many power grids have gradually formed AC–DC hybrid systems. Abnormal operations, such as DC blocking faults and generation trips, have led to several incidents of large frequency deviations. However, current simulation methods result in large errors when estimating the frequency regulation capacity of the system. This paper proposes a generic system frequency-response (SFR) model that can be used to estimate the dynamic frequency behavior of modern large-scale power systems. The limitations of the classical SFR model is first analyzed. Second, a generic SFR model with a more reasonable structure is presented, and the parameter-determination strategy is proposed using both the dynamic and steady-state data. Then, the generic SFR model is built and verified by a simulation case. Finally, a generic SFR model with satisfactory accuracy is established for the power grid in East China based on the measured disturbance data. The results show that the proposed model is promising for broad potential applications.

INDEX TERMS AC–DC hybrid system, DC blocking, frequency regulation, system frequency response (SFR), generic SFR model, parameter estimation.

I. INTRODUCTION

As some of the most important parameters of power systems, frequency and its dynamic characteristics are crucial for power system stability and control [1]. In the past, large frequency deviations in large-scale power grids have occurred rarely. Therefore, studies on the security and stability of the power system mainly focused on rotor angle stability and voltage stability, whereas frequency stability has received little attention. With the continuous development of ultra-high-voltage (UHV) AC and DC transmission technology, many power grids have gradually formed a large-scale long-distance UHV AC–DC hybrid system [2]–[4]. Abnormal operations, such as DC blocking faults and trips of generation, have led to several incidents of large frequency deviations in the world, including China and the UK [5], [6]. However, existing methods lack sufficient precision for frequency prediction, which poses a great threat to the safety and stable operation of power systems. Therefore, it is of great significance to conduct in-depth studies on frequency response modeling and prediction for modern large-scale power systems.

Currently, there are four methods for power system frequency-response (SFR) modeling and prediction: full model time-domain simulation, linearized models, artificial intelligence, and single-machine equivalent models. The full model time-domain simulation method is currently the most widely used for dynamic frequency calculation [7]. However, it takes all elements' dynamic characteristics into account, resulting in the largest computation workload. Moreover, owing to the large number of parameters involved, accurately setting all the parameters is a difficult task. The linearized model analysis method calculates dynamic frequency based on a partially linearized model [8]–[10]. Although it reduces the computation burden to a certain extent, it still encounters the same problems as the full model time domain simulation method when dealing with large scale power grid. The accuracy of the

The associate editor coordinating the review of this manuscript and approving it for publication was Dongbo Zhao.

artificial intelligence method relies on a large amount of measured data, currently making the method difficult to be promoted and applied in real power grids [11]–[13]. The single-machine equivalent model method has the least computation cost among the methods, and is suitable for online analysis [14]–[18]. The equivalent models mainly include the average system-frequency model (ASF) [14], [15], and SFR model [16], [18]. As the equivalent model with simple structure is capable of obtaining the analytical solution of the frequency response, it is applied to a wide variety of studies related to power system dynamics, such as demand response for frequency control [17], [19]–[21], and frequency-stability analysis [22]–[26].

In the SFR model, the prime mover-governor models of the generators are represented by a simplified reheat steam turbine-governor model. Thus, the classical SFR model is not suitable for modern power systems in which various types of governors and generators exist, such as hydraulic turbines and renewable power generators. Several studies on extended or improved SFR models have been recently performed. In [27], an improved average SFR model is proposed to evaluate the contribution of the inertial and droop responses from a wind farm to short-term frequency regulation. The role of electric vehicles contributing to the primary frequency response is investigated in [28] by using the simplified Great Britain power-system model, which is an improved SFR model. In [29], a convenient method is provided to unify the model for Type-3 wind turbines with a typical SFR model of synchronous generators to construct frequency-dynamics analysis for large-scale power systems. In [30], an extended SFR model with high-penetration wind power considering operating regions and wind-speed disturbance is proposed and verified through comparisons of the detailed model. However, most studies improve the SFR model for a particular purpose, such as integration of wind power or electric vehicles. In [18], an analytical method is proposed for aggregating the multi-machine SFR model into a single-machine model. However, the multi-machine SFR model and aggregated SFR model only include synchronous generators. Moreover, most of the improved SFR models are only verified by detailed model simulations. In other words, there is a lack of studies on universal SFR models with stronger adaptability and their validation in combination with the recorded disturbance data in a real large-scale power grid.

To address the gaps in the present literature, this work proposes a generic SFR model, which is verified using disturbance data recorded in the power grid of East China. The model structure is redesigned based on the classical SFR model, and the parameter determination strategy is also presented.

The remaining parts of this paper are organized as follows. Section II reviews the classical SFR model and presents the structure of the generic SFR model. Section III proposes the parameter determination of the generic SFR model. Section IV verifies the model via a detailed system simulation. Section V verifies the model using the disturbance data recorded in the power grid of East China. Finally, conclusions are made in Section VI.

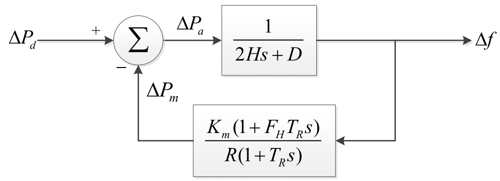

FIGURE 1. Classical SFR model.

II. GENERIC SFR MODEL STRUCTURE

A. CLASSICAL SFR MODEL STRUCTURE

The SFR model averages the machine dynamics in a multiple machines system into an equivalent single machine [16], the average system frequency is defined as the weighted summation of the machine speeds [14], i.e.,

$$f = \sum_{k=1}^{N} \rho_k f_k, \ \rho_k = H_k / \sum_{k=1}^{N} H_k \tag{1}$$

where f is the average system frequency in per-unit, f_k is the frequency or speed of the machine k in per-unit, H_k is the inertia constant of the machine k in seconds. The result is a representation of only the average system dynamics, while ignoring the inter-machine oscillations. As the fluctuation of SFR is usually small, the nonlinearity is not considered in the SFR model [16]–[18]. If the fluctuation of SFR is large, nonlinearity such as the position and rate limits of valves or gates should be considered.

By neglecting the nonlinear blocks and small time constants, a classical SFR model is proposed by P. M. Anderson and M. Mirheydar in [16] to derive an analytical expression of the average frequency dynamics of the power system, in which the generators are dominated by a reheat steam turbine.

The block diagram of the classical SFR model in [16] is shown in Fig. 1. Δf is frequency deviation, and ΔP_d is the power disturbance, which is positive for a sudden increase in generation or a sudden decrease in load, and negative for a sudden increase in load or sudden decrease in generation, i.e.,

$$\Delta P_d(t) = \Delta P_d \varepsilon(t), \quad \Delta P_d = \begin{cases} > 0, & \text{if generation increase} \\ & \text{or load decrease} \\ < 0, & \text{if load increase or} \\ & \text{generation decrease} \end{cases} \tag{2}$$

ΔP_m is the mechanical power deviation; ΔP_a is the accelerating power;$2H$ is the equivalent inertia constant of the generator in seconds; D is the equivalent damping factor; R is the droop setting of the governor; K_m is the mechanical power gain factor, such that K_m/R is the actual droop coefficient; T_R is the reheat time constant in seconds; and F_H is the fraction of total power generated by the high-pressure turbine. It can be observed from Fig.1 that the feedback loop includes

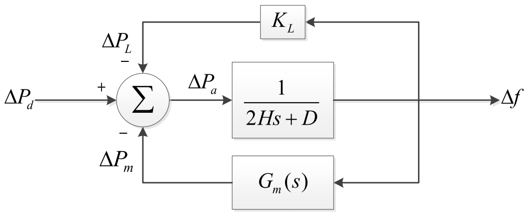

FIGURE 2. Interim SFR model.

two parts: the aggregate prime mover model and the governor model. The aggregate prime-mover model is described by a simplified reheat steam-turbine model, whereas the aggregate governor model is represented by the static droop coefficient. Therefore, the classic SFR model is only applicable to thermal power-generation systems with fast frequency modulation.

B. GENERIC SFR MODEL STRUCTURE

There are several problems when applying the classical SFR model to modern power systems. *1)* As it only considers the reheat steam turbine, it is not suitable for power systems integrated with hydro generation or renewable generation. *2)* The speed-governing system model is too simplified and may not represent its dynamic characteristic. *3)* There is no explicit consideration of the effect of load–frequency dependence. *4)* In the steam turbine-governor model, K_m and R, as well as F_H and T_R, cannot be uniquely determined.

Regarding the first and second problems, if extended with the dynamic models of the hydro generation and renewable generation, the SFR model will be too complicated to be used. Therefore, a uniform transfer function is proposed to describe the equivalent dynamics of the aggregate prime mover-governor [15], as shown in (3).

$$G_m(s) = \frac{\Delta P_m}{\Delta f} = \frac{\sum_{j=0}^{J} b_j s^{J-j}}{\sum_{i=0}^{I} a_i s^{I-i}}, \quad a_I = 1 \tag{3}$$

where a_i and b_j are the coefficients of the transfer function.

Regarding the third problem, a frequency dependent term of the load is added to SFR model [15], as shown in (4).

$$\Delta P_L = K_L \Delta f \tag{4}$$

where ΔP_L is the load power deviation; K_L is the frequency coefficient of the load. Thus, the model structure shown in Fig. 2 is obtained.

From Fig. 2, it can be determined that

$$[\Delta P_d - K_L \Delta f - G_m(s)\Delta f]\,\frac{1}{2Hs+D} = \Delta f \tag{5}$$

Hence, the whole transfer function of the system is

$$\frac{\Delta f}{\Delta P_d} = \frac{1}{2Hs + (D+K_L) + G_m(s)} \tag{6}$$

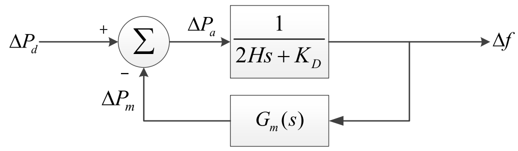

FIGURE 3. Generic SFR model.

It can be observed that D and K_L can be combined into one parameter, defined as

$$K_D = D + K_L \tag{7}$$

Therefore, the model shown in Fig. 3 can be obtained, which is called a generic SFR (G-SFR) model. In this model, the specific type of the prime mover-governor model is no longer involved, and thus, it is suitable for the power grids integrated with thermal, hydro, and renewable generation.

Regarding the fourth problem, the uniqueness of SFR model parameters will be solved in the Section III.

III. PARAMETER ESTIMATION OF G-SFR MODEL

A. PARAMETER ANALYSIS

According to (3), (6) and (7), the system transfer function between the frequency response and power disturbance can be deduced as follow:

$$\begin{aligned}\frac{\Delta f}{\Delta P_d} &= \frac{1}{(2Hs+K_D)+G_m(s)} \\ &= \frac{\sum_{i=0}^{I} a_i s^{I-i}}{(2Hs+K_D)\sum_{i=0}^{I} a_i s^{I-i} + \sum_{j=0}^{J} b_j s^{J-j}} \\ &= \frac{\sum_{i=0}^{I} a_i s^{I-i}}{2Ha_0 s^{I+1} + \sum_{i=0}^{I}\left(2Ha_{i+1} + K_D a_i + b_{i-(I-J)}\right) s^{I-i}}\end{aligned} \tag{8}$$

This can be written in the format of a uniform transfer function as (9).

$$G(s) = \frac{\sum_{i=0}^{I} B_i s^{I-i}}{\sum_{i=0}^{I+1} A_i s^{I+1-i}}, \quad B_I = 1 \tag{9}$$

where A_i and B_j are the coefficients of the system transfer function, which will be determined by parameter estimation based on measured data. It is noted that the number of system transfer-function parameters, excluding B_I, is $2I+2$, and the number of G-SFR parameters, excluding a_I, is $I+J+3$. If $J = I-1$, the number of system transfer function parameters will equal the number of G-SFR parameters, which will lead to the uniqueness of the G-SFR parameters. Here, $J = I-1$ means the order of the numerator is one less than that of the denominator, which is a very common situation. Then, the relationship between the system transfer-function parameters and G-SFR parameters can be obtained.

$$\begin{cases} B_i = a_i \quad (i = 0, \cdots, I-1) \\ A_0 = 2Ha_0 \\ A_1 = 2Ha_1 + K_D a_0 \\ A_{i+1} = 2Ha_{i+1} + K_D a_i + b_{i-1} \quad (i = 1, \cdots, I) \end{cases} \tag{10}$$

B. PARAMETER ESTIMATION BASED ON DYNAMIC DATA

1) According to the dynamic process of the power disturbance and the frequency response, the coefficients A_i and B_j in the transfer function (9) can be estimated by the least-squares method incorporated in MATLAB 2016b. The objective function is as follows:

$$\min_{\boldsymbol{\theta}=\boldsymbol{\theta}^*} E(\boldsymbol{\theta}) = \sum_{k=1}^{N} \left[f_{c,k}(\boldsymbol{\theta}) - f_{a,k}\right]^2 \tag{11}$$

where the subscript c represents the frequency-response data calculated using the G-SFR model, whereas the subscript a represents the actual or measured frequency response. The parameters $\boldsymbol{\theta}$ include A_i and B_j, i.e.,

$$\boldsymbol{\theta} = [A_0, \cdots, A_{I+1}, B_0, \cdots, B_J]^T \tag{12}$$

2) Based on (10), the parameters of the G-SFR model can be determined by

$$\begin{cases} H = \dfrac{A_0}{2B_0} \\ K_D = \dfrac{A_1 B_0 - A_0 B_1}{B_0^2} \\ a_i = B_i, \qquad (i = 0, \cdots, I-1) \\ b_j = \dfrac{A_{j+2}B_0^2 - A_0 B_0 B_{j+2} - A_1 B_0 B_{j+1} + A_0 B_1 B_{j+1}}{B_0^2}, \\ \qquad (j = 0, \cdots, J) \end{cases} \tag{13}$$

Therefore, with the estimated transfer-function parameters, the parameters in the G-SFR model can be determined uniquely.

C. PARAMETER ESTIMATION BASED ON DYNAMIC AND STEADY-STATE DATA

1) When dynamic response data are used to estimate the aforementioned coefficients in the transfer function (9), the error index is defined as the minimization of the dynamic errors. Therefore, it cannot guarantee zero or low steady-state error in frequency. As the steady-state values of frequency and power disturbance can be measured, the steady-state error is set to 0 as a constraint in this study, namely,

$$\lim_{t\to\infty} \left[\frac{\Delta P_d(t)}{\Delta f(t)}\right] = \frac{\Delta P_{d\infty}}{\Delta f_\infty} \tag{14}$$

where, $\Delta P_{d\infty}$ is the steady-state power disturbance, Δf_∞ is the steady-state frequency deviation.

As steady state indicates $s = 0$ for the transfer function, substituting $s = 0$ into (3) yields

$$K_G = \frac{\Delta P_{m\infty}}{\Delta f_\infty} = G_m(0) = b_J \tag{15}$$

This means that b_J is the frequency droop coefficient of the generator. Furthermore, from (13) and (15), we have

$$K_D + K_G = \frac{A_1 B_0 - A_0 B_1}{B_0^2} + \frac{A_{J+2}B_0^2 - A_1 B_0 + A_0 B_1}{B_0^2} = A_{I+1} \tag{16}$$

Then, substituting $s = 0$ into (8) and (9) yields

$$\frac{\Delta P_{d\infty}}{\Delta f_\infty} = \frac{1}{G(0)} = A_{I+1} = K_D + K_G \tag{17}$$

It can be observed that: (1) The system frequency-droop coefficients K_D and K_G jointly determine the steady-state value of the frequency response; (2) The sum of the two coefficients equals to A_{I+1}; (3) A_{I+1} can be determined directly by the steady-state data, so that A_{I+1} needs not to be estimated by the dynamic data.

2) According to the dynamic process of power disturbance and frequency response, the coefficients other than A_{I+1} in the transfer function (9) can be obtained using parameter estimation method, i.e.,

$$\boldsymbol{\theta} = [A_0, \cdots, A_I, B_0, \cdots, B_J]^T \tag{18}$$

3) Based on (10), (15), and (17), the parameters in the G-SFR model can be determined uniquely by

$$\begin{cases} H = \dfrac{A_0}{2B_0} \\ K_D = \dfrac{A_1 B_0 - A_0 B_1}{B_0^2} \\ K_G = b_J = \dfrac{\Delta P_{d\infty}}{\Delta f_\infty} - \dfrac{A_1 B_0 - A_0 B_1}{B_0^2} \\ a_i = B_i, \qquad (i = 0, \cdots, I-1) \\ b_j = \dfrac{A_{j+2}B_0^2 - A_0 B_0 B_{j+2} - A_1 B_0 B_{j+1} + A_0 B_1 B_{j+1}}{B_0^2}, \\ \qquad (j = 0, \cdots, J-1) \end{cases} \tag{19}$$

D. ORDER DETERMITION OF TRANSFER FUNCTION

As an important parameter of the G-SFR model, the order of transfer function $G_m(s)$, i.e., I in the previous section, should be determined.

This transfer function represents the equivalent relationship between total mechanical power deviation and system frequency deviation. It should be pointed out that, although the summation of the prime mover-governor transfer functions is of very high order. However, the average system frequency varies slowly. Therefore, a low-order transfer function may be obtained, in which only the slow modes are considered and the fast modes are neglected.

As there is no effective theoretical method for order determination, a trial and error method is used here. Trials were made in simulation systems such as IEEE 9-bus system, IEEE 39-bus system and the real power system such as East China Power Grid and Zhejiang Power Grid. In the following section, three transfer functions with first, second, and the

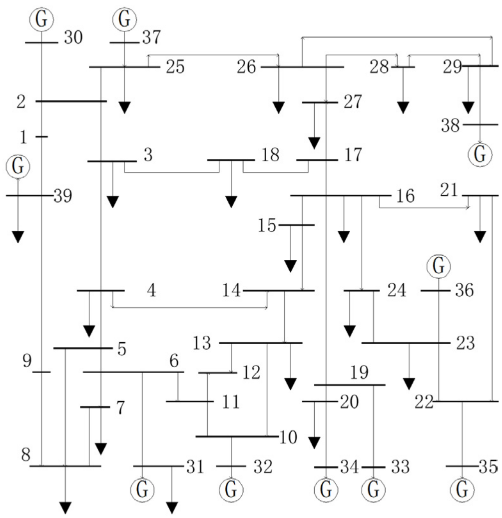

FIGURE 4. Configuration of the simulation system.

third orders are tested, i.e.,

$$\begin{cases} I=1, & G_m(s)=\dfrac{b_0}{a_0s+1} \\ I=2, & G_m(s)=\dfrac{b_0s+b_1}{a_0s^2+a_1s+1} \\ I=3, & G_m(s)=\dfrac{b_0s^2+b_1s+b_2}{a_0s^3+a_1s^2+a_2s+1} \end{cases} \quad (20)$$

To compare the G-SFR models with different orders, the errors of major indexes in system frequency response are defined as

$$\begin{cases} Error_{Initial\ slope} = \left|\dfrac{Slope_a - Slope_c}{Slope_a}\right| \times 100\% \\ Error_{extreme\ frequency} = \left|\dfrac{frequency_{Ma} - frequency_{Mc}}{frequency_{Ma}}\right| \\ \qquad \times 100\% \\ Error_{steady-state\ frequency} = \left|\dfrac{frequency_{\infty a} - frequency_{\infty c}}{frequency_{\infty a}}\right| \\ \qquad \times 100\% \end{cases} \quad (21)$$

where the subscript a represents the measured or actual value, the subscript c represents the value calculated with G-SFR model, the subscript M presents the minimum or maximum frequency in the dynamic process.

IV. VALIDATION OF THE G-SFR MODEL BY SIMULATION SYSTEMS

The simulation studies in an IEEE 39-bus system (as shown in Fig. 4) are reported here. To verify the effectiveness of the G-SFR model in the case of different generation, the simulation system includes hydro, thermal, and wind power units, as listed in Table 1. The simulations are based on the software PSD-BPA, which is a power system simulation software developed by the China Electric Power Research Institute and is widely used by power companies in China. The model structures of the prime mover and its governor in the hydro and thermal units are shown in Fig. 5 and Fig. 6, respectively. The introduction of these models can be found in Sections 5.1.2 and 5.1.3 of [31], respectively. Because the DFIG-based wind power generators operate in maximum power point tracking mode [32], they will not provide frequency regulation to the power system. Hence, the models of the wind power generator are not introduced here, but can be found in Section 6.2 of [31].

The total load of this system is 6192.8 MW when the system frequency is 50.00 Hz. We set three total load increase cases of +2.5%, +5.0% and +7.5%, respectively. The load increase occurred in some randomly selected buses, and the detailed amount is listed in Table 2.

TABLE 1. The settings of the generators in IEEE 39-Bus System.

Bus	Generator Type	Output power (MW)
31	Hydro unit	572.8
32		650
33		632
37		540
30	DFIG-based wind power unit	250
34		508
35	Thermal unit	650
36		560
38		830
39		1000

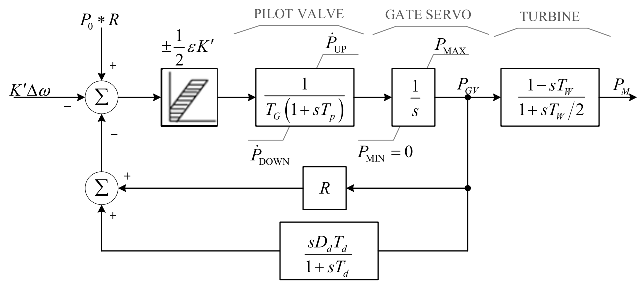

FIGURE 5. Model structures of the prime mover and its governor in a hydro unit.

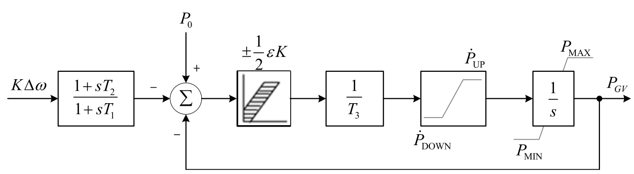

FIGURE 6. Model structures of the prime mover and its governor in a thermal unit.

TABLE 2. Settings of total load increase.

Case	Total increase	Load increase in individual bus
I	154.82 MW (+2.5%)	40.00 MW in Bus4, Bus8, Bus15; 34.82 MW in Bus20
II	309.64 MW (+5.0%)	60.00 MW in Bus3, Bus7, Bus16, Bus48; 69.64 MW in Bus20
III	464.46 MW (+7.5%)	120.00 MW in Bus7, Bus8, Bus16; 104.46 MW in Bus24

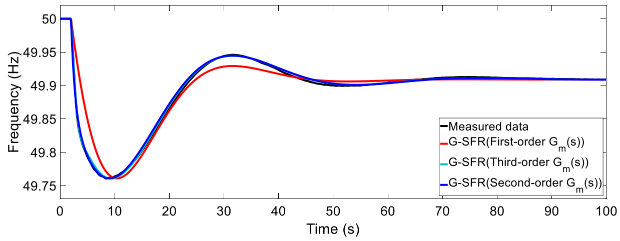

FIGURE 7. Comparisons of SFR among the actual data and the G-SFR models with different order.

TABLE 3. Errors of the G-SFR at different orders under +5.0% load increase.

Error	Order of $G_m(s)$		
	First order	Second order	Third order
$Error_{Initial\ slope}$	27.164%	0.582%	1.939%
$Error_{extreme\ frequency}$	0.017%	0.021%	0.022%
$Error_{steady\text{-}state\ frequency}$	0.027%	0.016%	0.046%

TABLE 4. Estimated parameters of the third-order G-SFR model.

Parameters	H/s	K_D	K_G	a_0	a_1	b_0
Estimation	5.473	14.230	13.158	71.354	23.054	-14.815

The system frequency response under Case II of +5% total load increase was used to estimate the coefficients in G-SFR. In this case, the frequency dropped to its minimum value of 49.761 Hz and finally reached 49.909 Hz. The results of the G-SFR with different orders are compared, Fig. 7 shows the SFR of G-SFR model with different orders, and the errors of major indexes are listed in Table 3.

Bases on the errors listed in Table 3, it could be seen that the second-order G_m(s) has the best results. In addition, according to the simulation results of frequency response with different scale systems and different disturbances, it is also found that the second-order G_m(s) is suitable to obtain satisfactory results of the system frequency response.

According to the parameter estimation method in Section III.C, the parameter A_3 is first determined according to the steady-state data, and the other parameters are then estimated by the least-square method in MATLAB 2016b based on the dynamic data. The parameter-estimation results of the third-order G-SFR model are shown in Table 4.

To validate the adaptability of the G-SFR model, the model obtained above is used to simulate the frequency response under different load increases as Case I and Case III listed in Table 2. The results are shown in Fig. 8 and the errors of the G-SFR models are listed in Table 5.

The following can be observed from Table 3, Table 5, Fig. 7, and Fig. 8: *1)* The output of G-SFR model are very close to the actual frequency responses; *2)* The minimum frequency obtained by the G-SFR model is accurate; *3)* The G-SFR model obtained in one case are adaptable to other cases; *4)* Using the second-order $G_m(s)$ in G-SFR is suitable to obtain satisfactory results.

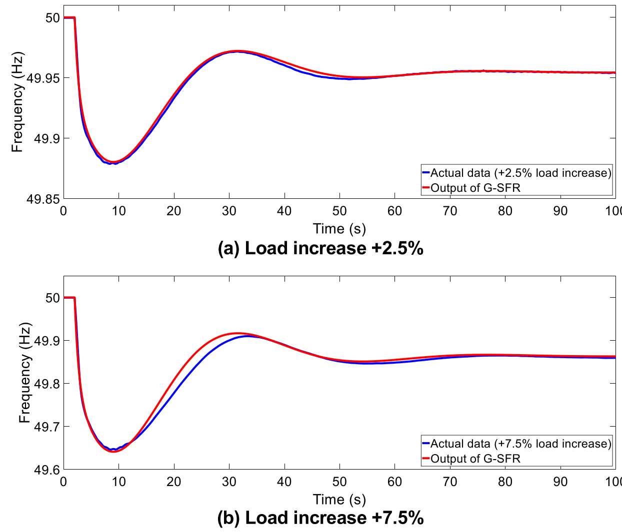

FIGURE 8. Comparisons of SFR among the actual data and the G-SFR model under different disturbances.

TABLE 5. Errors of the obtained G-SFR under different total load increase percentage.

Error	Percentage of total load increase		
	+2.5%	+5.0%	+7.5%
$Error_{Initial\ slope}$	2.420%	0.582%	1.304%
$Error_{extreme\ frequency}$	1.278%	0.021%	1.384%
$Error_{steady\text{-}state\ frequency}$	0.674%	0.016%	2.549%

V. VALIDATION OF THE G-SFR MODEL BY REAL SYSTEMS

Practical studies in the East China Power Grid are reported here. The power grid is a typical receiving-end power grid in China, which provides electricity for Shanghai city, Jiangsu province, Zhejiang province, Fujian province, and Anhui province. The East China Power Grid is the largest regional grid in China in terms of total electric load. The actual frequency-fluctuation data used in this section was recorded at 03:05:14 October 20, 2015. In 2015, there were a total of 241.8 GW thermal units, 20.18 GW hydro units, 14.01 GW nuclear units, 9.08 GW wind power units, and 3.77 GW photovoltaic units in the region of the East China Power Grid, and there were 7 DC lines that transmitted 31.76 GW electricity in total to the East China Power Grid. A single-pole blocking fault occurred in the Binjin DC Line, which resulted in a power shortage of approximately 3700 MW. Because the accident occurred at midnight, the total load was only approximately 160 GW before the accident. The system frequency decreased from 50.01 to 49.77 Hz, and then recovered to 49.87 Hz in this accident.

Based on this recorded data, we compare the outputs of G-SFR models with different orders as shown in Fig. 9, and the errors are listed in Table 6. It can be seen that although the East China Power Grid is quite a large power system, its frequency response can be represented by a low-order transfer function. The outputs of the G-SFR models with different

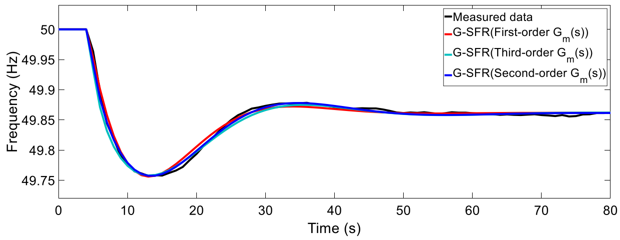

FIGURE 9. Comparisons of SFR among the measured data and the G-SFR models.

TABLE 6. Errors of the G-SFR model with different orders under field measured data in East China power grid.

Error	Order of $G_m(s)$		
	First order	Second order	Third order
$Error_{Initial\ slope}$	5.771%	2.763%	2.434%
$Error_{extreme\ frequency}$	0.548%	0.009%	0.249%
$Error_{steady\text{-}state\ frequency}$	0.056%	0.243%	0.255%

TABLE 7. Parameters of the G-SFR model for East China power grid.

Parameters	H/s	K_D	K_G	a_0	a_1	b_0
Estimation	9.767	2.561	5.943	353.37	36.41	395.49

orders are close to the measured one, whereas the G-SFR with second-order $G_m(s)$ is the best.

The parameters of the G-SFR with the second-order $G_m(s)$ were estimated and presented in Table 7 using the method presented in Section III.C. It can be seen from Fig. 9, Table 6, and Table 7 that: *1)* The frequency response using the G-SFR model fits the measured data quite well. *2)* The important parameters, including H, K_D, and K_G are all reasonable. For example, the East China Power Grid reported that parameter K_D ranged from 2.35 to 2.81 [5], and the estimated K_D was 2.561, which is within the range.

VI. CONCLUSION

A generic SFR model structure has been developed that is suitable for power systems including thermal, hydro, and renewable generation. The parameter-estimation strategy is then proposed, in which every parameter can be uniquely determined based on dynamic and steady-state data. The transfer function for equivalent prime mover-governor is suggested to be second-order. The effectiveness of the G-SFR model was verified by simulation cases. Furthermore, a G-SFR model of the power grid in East China was built based on the measured disturbance data, for which an ideal fitting effect was obtained.

REFERENCES

[1] P. Kundur, *Power System Stability and Control*. New York, NY, USA: McGraw-Hill, 1994.
[2] X. Zhou, J. Yi, R. Song, X. Yang, Y. Li, and H. Tang, "An overview of power transmission systems in China," *Energy*, vol. 35, no. 11, pp. 4302–4312, Nov. 2010.
[3] Y. Yu, J. Yang, and B. Chen, "The smart grids in China—A review," *Energies*, vol. 5, no. 5, pp. 1321–1338, May 2012.
[4] Y. Miao and H. Cheng, "An optimal reactive power control strategy for UHVAC/DC hybrid system in East China grid," *IEEE Trans. Smart Grid*, vol. 7, no. 1, pp. 392–399, Jan. 2016.
[5] H. Deng, B. L. Liu, W. Hua, H. Y. Wang, W. Z. Sun, and L. Ye, "Frequency stability analysis of East China Power Grid due to HVDC block," *Smart Power*, vol. 45, no. 8, pp. 39–44, Aug. 2017.
[6] (Aug. 9, 2019). *National Grid ESO*. Accessed: Sep. 6, 2019. [Online]. Available: https://www.nationalgrideso.com/document
[7] *PSS/E 33.0 Program Application Guide*, Siemens PTI, Schenectady, NY, USA, 2011.
[8] J. Dong, X. Ma, S. M. Djouadi, H. Li, and Y. Liu, "Frequency prediction of power systems in FNET based on state-space approach and uncertain basis functions," *IEEE Trans. Power Syst.*, vol. 29, no. 6, pp. 2602–2612, Nov. 2014.
[9] J. Hu, J. Cao, J. M. Guerrero, T. Yong, and J. Yu, "Improving frequency stability based on distributed control of multiple load aggregators," *IEEE Trans. Smart Grid*, vol. 8, no. 4, pp. 1553–1567, Jul. 2017.
[10] W. Ju, K. Sun, and R. Yao, "Simulation of cascading outages using a power-flow model considering frequency," *IEEE Access*, vol. 6, pp. 37784–37795, 2018.
[11] M. Djukanovic, D. Popovic, D. Sobajic, and Y.-H. Pao, "Prediction of power system frequency response after generator outages using neural nets," *IEE Proc. C Gener. Transmiss. Distrib.*, vol. 140, no. 5, p. 389, 1993.
[12] R.-F. Chang, C.-N. Lu, and T.-Y. Hsiao, "Prediction of frequency response after generator outage using regression tree," *IEEE Trans. Power Syst.*, vol. 20, no. 4, pp. 2146–2147, Nov. 2005.
[13] Q. Wang, C. M. Zhang, Y. Lu, Z. H. Yu, and Y. Tang, "Data inheritance-based updating method and its application in transient frequency prediction for a power system," *Int. Trans. Elect. Energy*, vol. 29, no. 6, pp. 1–16, Apr. 2019.
[14] M. Chan, R. Dunlop, and F. Schweppe, "Dynamic equivalents for average system frequency behavior following major distribances," *IEEE Trans. Power App. Syst.*, vols. PAS–91, no. 4, pp. 1637–1642, Jul. 1972.
[15] J. Liu, X. Wang, J. Lin, and Y. Teng, "A hybrid equivalent model for prediction of power system frequency response," presented at the IEEE Power Energy Soc. Gen. Meeting (PESGM), Aug. 2018.
[16] P. Anderson and M. Mirheydar, "A low-order system frequency response model," *IEEE Trans. Power Syst.*, vol. 5, no. 3, pp. 720–729, 1990.
[17] D. Aik, "A general-order system frequency response model incorporating load shedding: Analytic modeling and applications," *IEEE Trans. Power Syst.*, vol. 21, no. 2, pp. 709–717, May 2006.
[18] Q. Shi, F. Li, and H. Cui, "Analytical method to aggregate multi-machine SFR model with applications in power system dynamic studies," *IEEE Trans. Power Syst.*, vol. 33, no. 6, pp. 6355–6367, Nov. 2018.
[19] U. Rudez and R. Mihalic, "Monitoring the first frequency derivative to improve adaptive underfrequency load-shedding schemes," *IEEE Trans. Power Syst.*, vol. 26, no. 2, pp. 839–846, May 2011.
[20] P. Babahajiani, Q. Shafiee, and H. Bevrani, "Intelligent demand response contribution in frequency control of multi-area power systems," *IEEE Trans. Smart Grid*, vol. 9, no. 2, pp. 1282–1291, Mar. 2018.
[21] G. Benysek, J. Bojarski, R. Smolenski, M. Jarnut, and S. Werminski, "Application of stochastic decentralized active demand response (DADR) system for load frequency control," *IEEE Trans. Smart Grid*, vol. 9, no. 2, pp. 1055–1062, Mar. 2018.
[22] H. Yu, R. Bansal, and Z. Dong, "Fast computation of the maximum wind penetration based on frequency response in small isolated power systems," *Appl. Energy*, vol. 113, pp. 648–659, Jan. 2014.
[23] N. Nguyen and J. Mitra, "An analysis of the effects and dependency of wind power penetration on system frequency regulation," *IEEE Trans. Sustain. Energy*, vol. 7, no. 1, pp. 354–363, Jan. 2016.
[24] S. Liao, J. Xu, Y. Sun, W. Gao, X.-Y. Ma, M. Zhou, Y. Qu, X. Li, J. Gu, and J. Dong, "Load-damping characteristic control method in an isolated power system with industrial voltage-sensitive load," *IEEE Trans. Power Syst.*, vol. 31, no. 2, pp. 1118–1128, Mar. 2016.
[25] D. Ochoa and S. Martinez, "Fast-frequency response provided by dfig-wind turbines and its impact on the grid," *IEEE Trans. Power Syst.*, vol. 32, no. 5, pp. 4002–4011, Sep. 2017.
[26] H. Pulgar-Painemal, Y. Wang, and H. Silva-Saravia, "On inertia distribution, inter-area oscillations and location of electronically-interfaced resources," *IEEE Trans. Power Syst.*, vol. 33, no. 1, pp. 995–1003, Jan. 2018.

[27] H. Ye, W. Pei, and Z. Qi, "Analytical modeling of inertial and droop responses from a wind farm for short-term frequency regulation in power systems," *IEEE Trans. Power Syst.*, vol. 31, no. 5, pp. 3414–3423, Sep. 2016.
[28] Y. Mu, J. Wu, J. Ekanayake, N. Jenkins, and H. Jia, "Primary frequency response from electric vehicles in the great britain power system," *IEEE Trans. Smart Grid*, vol. 4, no. 2, pp. 1142–1150, Jun. 2013.
[29] J. Hu, L. Sun, X. Yuan, S. Wang, and Y. Chi, "Modeling of type 3 wind turbines with df/dt inertia control for system frequency response study," *IEEE Trans. Power Syst.*, vol. 32, no. 4, pp. 2799–2809, Jul. 2017.
[30] J. Dai, Y. Tang, Q. Wang, P. Jiang, and Y. Hou, "An extended SFR model with high penetration wind power considering operating regions and wind speed disturbance," *IEEE Access*, vol. 7, pp. 103416–103426, 2019.
[31] *User Manual of PSD-ST Transient Stability Program (V5.1.3)*, China Electr. Power Res. Inst., Beijing, China, 2018.
[32] A. Fernández-Guillamón, E. Gómez-Lázaro, E. Muljadi, and Á. Molina-García, "Power systems with high renewable energy sources: A review of inertia and frequency control strategies over time," *Renew. Sustain. Energy Rev.*, vol. 115, Nov. 2019, Art. no. 109369.

H. HUANG received the B.Eng. degree in electrical engineering from Hohai University, China, in 2011, and the M.S. degree in electrical engineering from the University of Strathclyde, U.K., in 2013. She is currently pursuing the Ph.D. degree with the Huazhong University of Science and Technology, China.

Her research interests include modeling and control of power grids with renewable generation.

P. JU (Senior Member, IEEE) received the B.Eng. and M.S. degrees in electrical engineering from Southeast University, China, in 1982, 1985, respectively, and the Ph.D. degree in electrical engineering from Zhejiang University, China, in 1988.

From 1994 to 1995, he was an Alexander-von-Humboldt Fellow with the University of Dortmund, Germany. He is currently a Professor of electrical engineering with Hohai University and Zhejiang University, China. He has published six books and over 300 journal articles. His research interests include modeling and control of power systems and smart grids with renewable generation.

Prof. Ju was awarded the Scientific Funds for Outstanding Young Scientists of China, in 2007, and the National Science and Technology Progress Award of China, in 2017.

Y. JIN received the B.Eng., M.S., and Ph.D. degrees in electrical engineering from Hohai University, Nanjing, China, in 2002, 2006, and 2012, respectively.

He is currently an Associate Professor of electrical engineering with the College of Energy and Electrical Engineering, Hohai University. His research interests are modeling and control of renewable power generation.

X. YUAN (Senior Member, IEEE) received the B.Eng. degree from Shandong University, China, in 1986, the M.Eng. degree from Zhejiang University, China, in 1993, and the Ph.D. degree from the Federal University of Santa Catarina, Florianopolis, Brazil, in 1998, all in electrical engineering.

He was with Qilu Petrochemical Corporation, China, from 1986 to 1990, where he was involved in the commissioning and testing of relaying and automation devices in power systems, adjustable speed drives, and high-power UPS systems. From 1998 to 2001, he was a Project Engineer with the Swiss Federal Institute of Technology Zurich, Zurich, Switzerland, where he worked on flexible-AC-transmission-systems and power quality. From 2001 to 2008, he was with GE GRC Shanghai as the Manager of the Low Power Electronics Laboratory. From 2008 to 2010, he was with GE GRC US as an Electrical Chief Engineer. He is currently a Professor of electrical engineering with the Huazhong University of Science and Technology, Wuhan, China. His research field involves stability and control of power system with multi machines multi converters, control and grid-integration of renewable energy generations, and control of high-voltage DC transmission systems.

Prof. Yuan is also a Distinguished Expert of National Thousand Talents Program of China and the Chief Scientist of National Basic Research Program of China (973 Program). He received the First Prize Paper Award from the Industrial Power Converter Committee of the IEEE Industry Applications Society, in 1999.

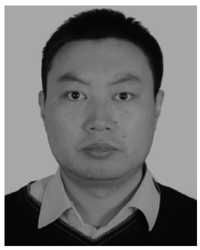

C. QIN (Member, IEEE) received the B.Eng. degree in electrical engineering from the Nantong Institute of Technology, China, in 2002, and the M.S. and Ph.D. degrees in electrical engineering from Hohai University, Nanjing, China, in 2005 and 2013, respectively.

He is currently an Associate Professor of electrical engineering with Hohai University. His research interests are modeling and control of renewable power generations.

X. PAN (Member, IEEE) received the B.Eng. and M.S. degrees in electrical engineering from Hohai University, China, in 1994 and 2000, respectively, and the Ph.D. degree from the Zhejiang University, China, in 2008.

She is currently a Professor of electrical engineering with the College of Energy and Electrical Engineering, Hohai University, Nanjing, China. Her research interests include modeling of the renewable power generation and analysis and control of power systems.

X. ZANG received the B.Eng. degree in electrical engineering from Hohai University, China, in 2016, where he is currently pursuing the M.S. degree in electrical engineering. His research interest is frequency stability analysis of power systems.